Lattice Dynamics of MgO at High Pressure: Theory and Experiment

Subrata Ghose,[1] Michael Krisch,[2] Artem R. Oganov,[3] Alexandre Beraud,[2] Alexey Bosak,[2] Revansidha Gulve,[4] Raghunandan Seelaboyina,[4] Hexiong Yang,[4] and Surendra K. Saxena[4]

[1]*Mineral Physics Group, Box 351310, University of Washington, Seattle, Washington 98195, USA*
[2]*European Synchrotron Radiation Facility, Boîte Postale 220, F-38043 Grenoble Cedex, France*
[3]*Laboratory of Crystallography, Department of Materials, ETH Zurich, CH-8093 Zurich, Switzerland*
[4]*Center for Study of Matter at Extreme Conditions, Florida International University Park, VH-140, Miami, Florida 33199, USA*

(Received 27 February 2005; published 26 January 2006)

The longitudinal acoustic and optical phonon branches along the Γ-X direction of MgO at 35 GPa have been determined by inelastic x-ray scattering using synchrotron radiation and a diamond-anvil cell. The experimentally observed phonon branches are in remarkable agreement with *ab initio* lattice dynamics results. The derived thermodynamic properties, such as the specific heat C_V and the entropy S are in very good accord with values obtained from a thermodynamically assessed data set involving measured data on molar volume, heat capacity at constant pressure, bulk modulus and thermal expansion.

DOI: 10.1103/PhysRevLett.96.035507 PACS numbers: 62.50.+p, 63.20.−e, 78.70.Nx

The experimental determination of the phonon dispersion at high pressure constitutes an important ingredient for the characterization of the physical properties of materials in extreme conditions. It gives access to valuable quantitative information concerning elasticity, thermodynamic properties, and the dynamics of phase instabilities. Furthermore, the experimental data provide important tests for the accuracy of theoretical lattice dynamical models. Among these the most advanced ones are *ab initio* quantum mechanical calculations, using density-functional perturbation theory. Critical inputs are the appropriate choice of the potential (all-electron or pseudopotential approaches) and the correct description of the exchange-correlation term. If a good agreement with the experimental phonon dispersion is observed, these calculations can then be used with increased confidence to describe the physical properties such as elastic and dielectric constants, etc., and thermodynamic properties, such as specific heat, entropy, etc., at very high pressures beyond the reach of current experimental methods.

Until recently, inelastic neutron scattering (INS) has been extensively used to study the phonon dispersion throughout the Brillouin zone of the crystal. Phonon dispersion has been determined in a large number and variety of crystals by INS as well as their temperature dependence, particularly in connection with phase transitions and soft modes, i.e., phonons whose frequency approaches zero as T approaches the transition temperature T_c. However, the weak interaction of neutrons with matter and the typical size of neutron beams require the use of relatively large (ca. 1 cm^3) single crystals, which puts an upper limit for the measurement of phonon dispersion at high pressure at present to about 10–15 GPa by INS [1]. The technique of inelastic x-ray scattering (IXS) in conjunction with third generation synchrotron sources now makes it possible to measure the phonon dispersion at high pressures up to about 50 GPa in crystals tens of microns in size mounted in a diamond-anvil cell. Using He as a pressure transmitting medium, the phonon dispersions in single crystals of Ar to 20 GPa [2] and in hcp-Co to 39 GPa [3] have thus been recorded. Without a pressure transmitting medium, pressures as high as 112 GPa were reached on polycrystalline samples of iron and iron containing compounds [4,5].

In this Letter, we present the experimental determination of the longitudinal acoustic (LA) and optical (LO) phonon branches along the Γ-X direction in MgO at 35 GPa, utilizing inelastic x-ray scattering, and the comparison with *ab initio* calculations. Our choice of MgO is motivated by its importance in various fields of research. The material is regarded as the prototype oxide due to its simple structure and the large stability field (in pressure and temperature) of the NaCl structure [6]. Moreover, it is considered as a pressure calibration standard for high-pressure sciences [7]. Furthermore, MgO is an important ceramic for industrial applications, and of great interest for Earth sciences, since it is a major mineral phase of the Earth's lower mantle [8].

A doubly polished single crystal of MgO of (100) orientation, 30×50 μm size and a thickness of 20 μm was loaded in a diamond-anvil cell with He as pressure transmitting medium along with a few very small fragments of ruby for the pressure calibration. The pressures were determined from the ruby R_1 fluorescence line and were accurate to ± 0.5 GPa. The IXS experiment was performed on beamline ID28 at the European Synchrotron Radiation Facility, Grenoble, France. X rays from an undulator source were monochromatized by a silicon (111) double crystal and a backscattering very high-energy resolution monochromator, utilizing the silicon (999) reflection order at 17 794 eV. A cylindrical mirror in conjunction with a dynamically bent multilayer provided a focus of 25×60 μm H (horizontal) $\times$ V (vertical) full width at half maximum (FWHM) at the sample position. The scattered

photons were energy analyzed by a spherical crystal analyzer spectrometer operated in Rowland geometry and at the same reflection order as the monochromator. In this configuration the overall energy resolution amounted to 3 meV. The momentum transfer, $\mathbf{Q} = 2\mathbf{k_o}\sin(\theta_s/2)$, where $\mathbf{k_o}$ is the wave vector of the incident photons and θ_s, the scattering angle, was selected by rotating the analyzer arm in the horizontal plane. The Q resolution was set to $0.25 \times 0.8\ \mathrm{nm}^{-1}$ ($H \times V$), and the IXS scans were performed in a constant-Q mode. The data were normalized to the intensity of the incident beam. Further details of the setup can be found elsewhere [9].

Theoretical phonon dispersion curves were calculated exactly as in a previous work on MgO [10]. We used density-functional perturbation theory [11] as implemented in the pseudopotential plane wave code ABINIT [12]. The advantage of this approach over the often used finite-displacement methods is that we can explicitly treat the long-range Coulomb interactions; this allows one to get, e.g., the correct LO-TO splittings in ionic solids. For exchange-correlation we used the local density approximation [13]. The effect of core electrons on valence orbitals was described by Troullier-Martins [14] pseudopotentials, fully nonlocal and including partial core corrections [15]. Athermal structural optimizations were performed at 0.1 MPa (ambient pressure) and 35 GPa, and lattice dynamics were analyzed for the resulting structures. All calculations were done on a primitive 2-atom unit cell; the Brillouin zone was sampled with $8 \times 8 \times 8$ Monkhorst-Pack meshes, and a cutoff of 40 Ha was used for plane waves. Response functions were calculated on a $4 \times 4 \times 4$ grid of $\mathbf{q}$ points in the Brillouin zone, including the Γ point. Interpolating the dynamical matrices calculated on this grid throughout the Brillouin zone allows the calculation of the phonon frequencies at any given wave vector. For more details on methodology and convergence tests, see previous work [10]. Our results for MgO at 0.1 MPa are in good agreement with previous calculations by Schütt *et al.* [16] and Karki *et al.* [17] as well as INS experiments [18], whereas theoretical results of Drummond and Ackland [19] display significant differences, in particular, for the longitudinal branches along the Γ-X direction. Similar calculations on other systems have been recently reported as well [20,21].

Figure 1 shows representative IXS spectra. The spectra are dominated by a strong elastic line at low reduced momentum transfer (close to the Γ point) as a result of the proximity to the Bragg peak and the sample quality. Nevertheless, the inelastic feature at positive (negative) energies corresponding to energy loss (gain), and associated with the creation (annihilation) of a phonon, is clearly visible. With increasing phonon energy the phonon intensity rapidly drops, and consequently the high-energy optical phonons display a much lower count rate. The experimental spectra are fitted to a model function, composed of a set of Lorentzian functions, constrained by the Bose occupation factor.

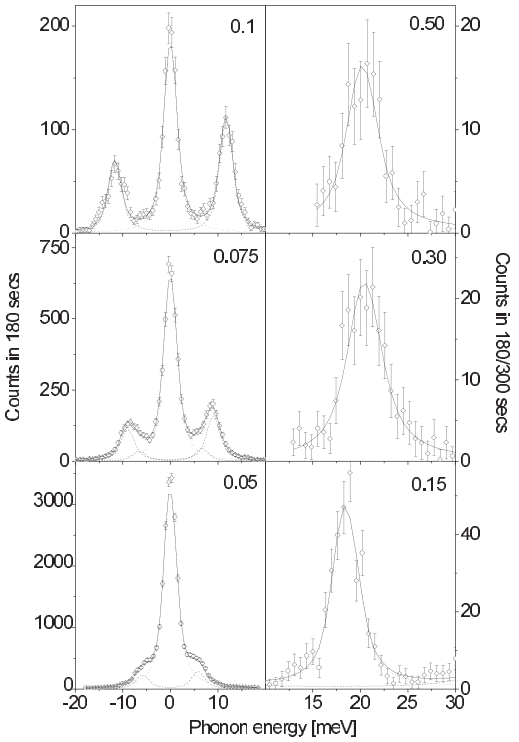

FIG. 1. Representative IXS spectra of MgO at 35 GPa along the $[\xi 00]$ (Γ-X) direction at reduced momentum transfer values as indicated in the individual panels. The experimental data are shown together with their best fits. Solid line: total fit; dotted line: elastic contribution; dashed lines: inelastic contributions. The energy scale in the panels on the right side is only valid for the spectrum at $\xi = 0.15$; the spectra at $\xi = 0.3$ and $\xi = 0.5$ are offset by 15 meV and 35 meV, respectively.

Figure 2 shows the resulting dispersion of the LA and LO branch along Γ-X, together with the *ab initio* results. We note a remarkable agreement between theory and experiment. In particular the over-bending of the LA branch and the minimum of the LO branch between $\xi = 0.7$ and 0.9, signifying an anticrossing, is well reproduced. This feature is not observed at ambient pressure, thus indicating that besides the expected overall increase of the phonon frequencies with pressure, there are already significant changes in the interatomic interactions at 35 GPa. This is further emphasized by inspection of the calculated complete phonon dispersion scheme and the derived phonon density of states (PDOS), which are reported in Fig. 3.

The left panel of Fig. 3 shows the theoretical results at $P = 0.1$ MPa, together with experimental results, obtained by INS [18]. Heat capacity C_V and entropy S, obtained from the calculated PDOS, agree well with thermochemical measurements [22]: $C_V = 36.58$ (36.87)and $S = 26.80$ (27.13) $\mathrm{J\,mol^{-1}\,K^{-1}}$ from theory [10] (experiment at 0.1 MPa and 300 K). At 35 GPa, we observe, as already

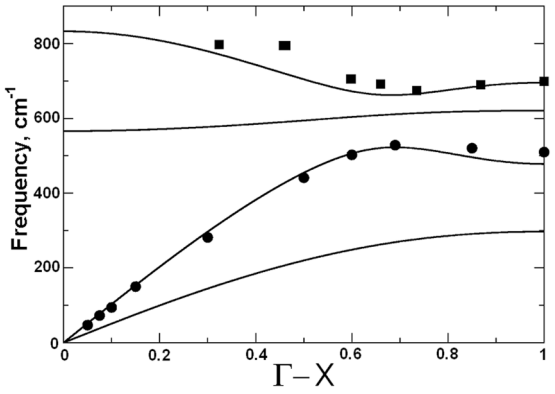

FIG. 2. Phonon dispersion curves of MgO along Γ-X direction at 35 GPa. Experimental data (this work) are shown by symbols (filled circles: LA branch; filled squares: LO branch). The error bars are smaller than the symbol size. Results of the *ab initio* calculations are shown as solid lines.

mentioned, a strong overall increase of phonon frequencies. Second, the structure of the phonon dispersion curves changes significantly—especially along the Γ-X and L-W directions. Third, the density of states develops a more complicated structure than at low pressure. The latter is due to a stronger over-bending of the acoustic branches, in particular, along the Γ-K-X and L-X directions, and changes in the dispersion of the optical branches. Furthermore, signatures of individual phonon branches

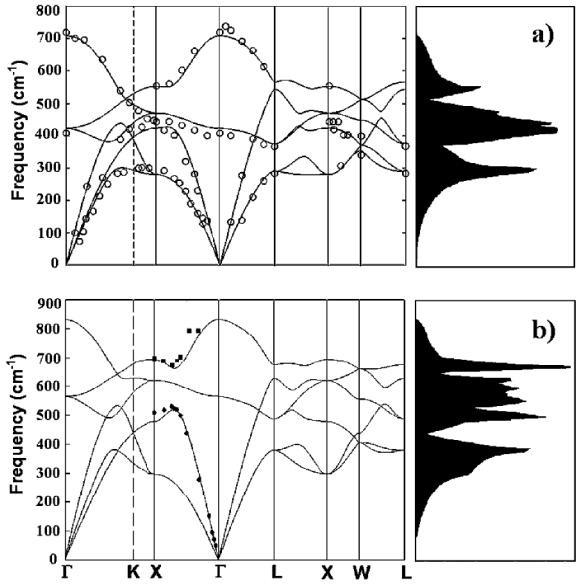

FIG. 3. Phonon dispersion curves and phonon density of states of MgO in the NaCl structure: (a) at 0.1 MPa, (b) at 35 GPa. Experimental data at 0.1 MPa [18] is shown in (a) as open circles. The present IXS results are shown by filled symbols (b). Results of the *ab initio* calculations are shown as solid lines.

are more visible at higher pressure, since the phonon spectrum is extended to higher frequencies (830 cm^{-1} instead of 710 cm^{-1}).

The fact that characteristic features in the phonon dispersion are well reproduced by *ab initio* calculations gives us confidence that *ab initio* predictions of thermodynamic properties of MgO at high pressure will be accurate. This is confirmed by the thermodynamic analysis that we present below.

The Gibbs free energy of a solid is given by

$$\Delta G(P,T) = \Delta H_T^0 - T\Delta S_T^0 + \int_1^P \Delta V(P,T)dP$$

where ΔH_T^0 and ΔS_T^0 are the standard enthalpy and entropy of formation, respectively, at temperature T and a pressure of 1 atm, and V is the molar volume at a given pressure and temperature. The determination of a thermodynamic property at high pressure requires us to experimentally determine the thermal expansion and the bulk modulus which are recast into an equation of state (EOS). Such EOS data are very few and, when available, the data usually require large extrapolation. Thermodynamic properties at high pressure may then be calculated from a combination of calorimetric data at 1 bar and the volume integral with changing pressure and temperature [23]. The high-pressure heat capacity is obtained by suitably differentiating the Gibbs free energy. Using the thermodynamic data from Saxena *et al.* [23] we obtain $C_V = 30.04(\pm 5)$ and $\Delta S = 20.68(\pm 1)$ J mol^{-1} K^{-1}. The indicated errors can be considered as an upper bound, and are estimated from the individual errors of all the input parameters (bulk modulus, thermal expansion, molar volume, and heat capacity). From the calculated PDOS at 35 GPa we determine $C_V = 31.71$ and $S = 20.04$ J mol^{-1} K^{-1}. The two data sets match within the errors of experimental data.

In summary, we present the first, and very successful, test of the ability of modern theory to reproduce experimental data on lattice dynamics of inorganic compounds measured by inelastic x-ray scattering in microcrystals under very high pressure. The success of this rather stringent test must enhance the confidence in computational techniques. We also believe that expanding such tests to other, more complex, systems could be beneficial for the development of both theory and experiment. These tests, validating the approximations made in the calculations, will allow the reliable determination of the thermodynamic properties of materials at high pressure, which are otherwise extremely difficult to assess by experimental methods.

S. G. is grateful to Dr. Narayani Choudhury, Bhabha Atomic Research Centre for suggesting the use of IXS for the study of lattice dynamics at high pressure. A. R. O. would like to thank the Centro Svizzero di Calcolo Scientifico (Manno) for computing facilities and ETH Zurich for funding. The work at CeSMEC was sup-

ported by a NSF grant (No. DMR-0231291). Dean Gibson is acknowledged for his help in the preparation of the diamond-anvil cell.

[1] S. Klotz and M. Braden, Phys. Rev. Lett. **85**, 3209 (2000).
[2] F. Occelli, M. Krisch, P. Loubeyre, F. Sette, R. Le Toullec, C. Masciovecchio, and J. P. Rueff, Phys. Rev. B **63**, 224306 (2001).
[3] D. Antonangeli, M. Krisch, G. Fiquet, D. L. Farber, C. M. Aracne, J. Badro, F. Occelli, and H. Requardt, Phys. Rev. Lett. **93**, 215505 (2004).
[4] G. Fiquet, J. Badro, F. Guyot, H. Requardt, and M. Krisch, Science **291**, 468 (2001); G. Fiquet, J. Badro, F. Guyot, Ch. Bellin, M. Krisch, D. Antonangeli, H. Requardt, A. Mermet, D. Farber, C. Aracne-Ruddle, and J. Zhang, Phys. Earth Planet. Inter. **143**, 5 (2004).
[5] D. Antonangeli, F. Occelli, H. Requardt, J. Badro, G. Fiquet, and M. Krisch, Earth Planet. Sci. Lett. **225**, 243 (2004).
[6] T. S. Duffy, R. J. Hemley, and H.-K. Mao, Phys. Rev. Lett. **74**, 1371 (1995).
[7] W. Utsumi, D. J. Weidner, and R. C. Liebermann in *Properties of Earth and Planetary Materials at High Pressures and Temperatures*, edited by M. H. Manghnani and T. Yagi (American Geophysical Union, Washingon, D.C., 1998), pp. 327–333.
[8] D. L. Anderson, *Theory of the Earth* (Blackwell Scientific, Boston, 1989).
[9] M. Krisch, J. Raman Spectrosc. **34**, 628 (2003).
[10] A. R. Oganov, M. J. Gillan, and G. D. Price, J. Chem. Phys. **118**, 10 174 (2003).
[11] For a review, see S. Baroni, S. de Gironcoli, A. Dal Corso, and P. Gianozzi, Rev. Mod. Phys. **73**, 515 (2001).
[12] X. Gonze, J.-M. Beuken, R. Caracas, F. Detraux, M. Fuchs, G.-M. Rignanese, L. Sindic, M. Verstraete, G. Zerah, F. Jollet, M. Torrent, A. Roy, M. Mikami, Ph. Ghosez, J.-Y. Raty, and D. C. Allan, Comput. Mater. Sci. **25**, 478 (2002); ABINIT is a common project of the Université Catholique de Louvain, Corning Inc., and other contributors (http://www.abinit.org). Technical details on the computation of responses to atomic displacements and homogeneous electric fields can be found in the paper by X. Gonze, Phys. Rev. B **55**, 10 337 (1997), and the subsequent computation of dynamical matrices, Born effective charges, dielectric permittivity tensors, and interatomic force constants was described by X. Gonze and C. Lee, Phys. Rev. B **55**, 10 355 (1997).
[13] J. P. Perdew and Y. Wang, Phys. Rev. B **45**, 13 244 (1992).
[14] N. Troullier and J. L. Martins, Phys. Rev. B **43**, 1993 (1991).
[15] S. G. Louie, S. Froyen, and M. L. Cohen, Phys. Rev. B **26**, 1738 (1982).
[16] O. Schütt, P. Pavone, W. Windl, K. Karch, and D. Strauch, Phys. Rev. B **50**, 3746 (1994).
[17] B. B. Karki, R. M. Wentzcovitch, S. de Gironcoli, and S. Baroni, Phys. Rev. B **61**, 8793 (2000).
[18] G. Peckham, Proc. Phys. Soc. London **90**, 657 (1967); M. J. L. Sangster, G. Peckham, and D. H. Saunderson, J. Phys. C **3**, 1026 (1970).
[19] N. D. Drummond and G. J. Ackland, Phys. Rev. B **65**, 184104 (2002).
[20] A. R. Oganov and S. Ono, Nature (London) **430**, 445 (2004).
[21] A. R. Oganov, M. J. Gillan, and G. D. Price, Phys. Rev. B **71**, 064104 (2005); A. R. Oganov and S. Ono, Proc. Natl. Acad. Sci. U.S.A. **102**, 10 828 (2005).
[22] R. A. Robie and B. S. Hemingway, "*Thermodynamic Properties of Minerals and Related Substances at 289.15 K and 1 bar (105 Pascals) Pressure and at Higher Temperatures*," U.S. Geological Survey Bulletin No. 2131, 1995.
[23] S. K. Saxena, N. Chatterjee, Y. Fei, and G. Shen in *Thermodynamic Data on Oxides and Silicates* (Springer Verlag, Berlin, 1993), p. 428.